aminimide inhibitor was able to make nearly all the interactions with the enzyme that corresponding dipeptide inhibitors make. Although the aminimide contains an extra backbone atom relative to conventional amino acids, the carbonyl groups of the peptidomimetic make the same hydrogen bonds, and the side chains of the aminimide dipeptide analog bind to the same subsites on the enzyme.

REFERENCES AND NOTES

1. S. E. Cwirlay, E. A. Peters, R. W. Barrett, W. J. Dower, *Proc. Natl. Acad. Sci. U.S.A.* **87**, 6378 (1990); J. J. Devlin, L. C. Panganiban, P. E. Devlin, *Science* **249**, 404 (1990).
2. J. K. Scott and G. P. Smith, *Science* **249**, 386 (1990); H. M. Geysen, S. J. Rodda, T. J. Mason, Eds., *CIBA Found. Symp.* **119** (1986); M. A. Gallop, R. W. Barret, W. J. Downer, S. P. Fodor, E. M. Gordon, *J. Med. Chem* **37**, 1233 (1994).
3. D. Ringe, unpublished results.
4. A. Amour, A. Collet, C. Dubar, M. Reboud-Ravaux, *Int. J. Peptide Protein Res.* **43**, 297 (1994); A. Aubury *et al.*, *ibid.*, p. 305.
5. D. L. Hughes, L. C. Sieker, J. Beith, J.-L. Dimicoli, *J. Mol. Biol.* **162**, 645 (1982); A. Renaud, P. Lestienne, D. L. Hughes, J. Bieth, J.-L. Dimicoli, *J. Biol. Chem.* **258**, 8312 (1983).
6. D. Ringe and G. A. Petsko, in *New Perspectives in Drug Design*, P. M. Dean, G. Jolles, C. G. Newton, Eds. (Academic Press, New York, 1995), pp. 89–118.
7. D. M. Shotton and H. C. Watson, *Nature* **225**, 811 (1970).
8. Both the aminimide and the dipeptide inhibitor were prepared by total synthesis and confirmed by infrared spectroscopy (IR), ^{1}H nuclear magnetic resonance (NMR), ^{13}C NMR, and high-resolution mass spectroscopy. Aminimides can be synthesized readily in high yield by easily automated procedures (J. C. Hogan Jr., international patent PCT/US93/0624).
9. We measured rates in aqueous solutions containing 0.1 M Hepes (pH 7.5), 0.5 M NaCl, 10 μM HCl, and 10% dimethyl sulfoxide (DMSO), using either MeO-Suc-Ala-Pro-Val-PNA (where Me is a methyl group, Suc is succinyl, and PNA is *p*-nitroanilide) or Suc-$(Ala)_3$-PNA as substrate. TLMI has a value for K_i of 26 μM, but for the Leu-Phe dipeptide, no measurable inhibition could be obtained at the maximum solubility of 20 μM. Although the aminimide inhibitor is soluble in water at this concentration, DMSO was used for consistency with earlier studies.
10. PPE (Worthington Biochemicals; 96.5% pure) was used without further purification. A 4 mM (200x K_i) stock solution of the aminimide inhibitor in acetonitrile was prepared. Elastase crystals were grown as described [L. Sawyer *et al.*, *J. Mol. Biol.* **118**, 137 (1978)]. Crystals of PPE were transferred to 1 ml of mother liquor (30 mM sodium sulfate and 10 mM sodium acetate, pH 5.0). Slowly, 50 μl of the aminimide inhibitor solution was added. Twenty-four hours later, an additional 50 μl was added. The crystal was mounted in a sealed quartz capillary tube.
11. C. Mattos, D. A. Giammona, G. A. Petsko, D. Ringe, *Biochemistry* **34**, 3193 (1995).
12. W. Bode *et al.*, *EMBO J.* **5**, 2453 (1986).
13. The program X-PLOR [A. T. Brünger, M. Karplus, G. A. Petsko, *Acta Cryst* **A45**, 50 (1989)] was used for refinement. The initial protein model was an unpublished structure of native elastase that had been refined to an *R* factor of 17.8% at 1.6 Å resolution. An initial rigid body refinement of this model with water and bound ions removed, followed by positional refinement, gave an *R* factor of 25.9% against all measured data for the PPE-TLMI complex. An electron density map with coefficients $2F_o$ (observed) $- F_c$ (calculated) was calculated, and protein side chains were adjusted. Electron density indicating the presence of inhibitor bound in the active site was seen. Another round of positional and independent *B* factor refinement was performed, and 122 water molecules, one sulfate ion, and one calcium ion were added to the model. After an additional round of refinement, a model of the inhibitor was added to the protein model on the basis of a difference electron density map with coefficients $F_o - F_c$. The electron density clearly showed the position of the TFA, Leu, and the Iso. portions of the inhibitor. Electron density for the carbonyl group uniquely positions the backbone of the inhibitor in the region of the MBA residue. The orientation of the methyl group on the quaternary nitrogen, which determines the chirality of that nitrogen, was initially unclear in the electron density map. Therefore, a model of the *S* isomer was used in a conformation in which the methyl group was eclipsed with the carbonyl oxygen of the Leu residue. Because this model did not refine well, the alternate conformation was tried in which the methyl group was placed trans to the carbonyl oxygen. This operation converts the *S* isomer into the *R* isomer. This model fitted the observed electron density better and refined smoothly. This result implies that the *R* configuration at this nitrogen is the preferred conformation that binds to the enzyme. Subsequently, several additional rounds of refinement added and removed water molecules. To check on the proper placement of the inhibitor in later stages of refinement, the inhibitor atoms were removed from the model and the model bias was removed from the phases with the program SHAKEUP (A. Lavie, K. N. Allen, R. L. Rardin, personal communication). Subsequent positional and *B* factor refinements followed by difference electron density map calculations indicated that the inhibitor had been placed correctly. The final *R* factor is 19.2% for a model that contains 1829 protein atoms, 1 calcium ion, 1 sulfate ion, and 134 water molecules plus the TLMI inhibitor.
14. All sequence numbering is sequential numbering in elastase.
15. C. Mattos, B. Rasmussen, X. Ding, G. A. Petsko, D. Ringe, *Nature Struct. Biol.* **1**, 55 (1994).
16. C. Mattos and D. Ringe, in *QSAR in Drug Design: Theory, Methods and Applications*, H. Kubinyi, Ed. (ESCOM Science Publishers, Leyden, Netherlands, 1993), pp. 226–254.
17. I. L. de la Sierra, E. Papamichael, C. Sakrellos, J.-L. Dimicoli, T. Prangé, *J. Mol. Recognit.* **3**, 36 (1990). The atomic coordinates of this structure were taken from the Brookhaven Protein Databank [F. C. Bernstein, T. F. Koetzle, G. J. B. Williams, E. F. Meyer Jr., *J. Mol. Biol.* **112**, 535 (1977)].
18. W. Kabsch, *J. Appl. Crystallogr.* **21**, 916 (1988).
19. Abbreviations for the amino acid residues are as follows: A, Ala; C, Cys; D, Asp; E, Glu; F, Phe; G, Gly; H, His; I, Ile; K, Lys; L, Leu; M, Met; N, Asn; P, Pro; Q, Gln; R, Arg; S, Ser; T, Thr; V, Val; W, Trp; and Y, Tyr.
20. P. J. Kraulis, *J. Appl. Crystallogr.* **24**, 946 (1991).

21. Research was supported (in part) by the Biophysics Program at Brandeis University (NIH T32GMO7596) and the Lucille P. Markey Charitable Trust. E.P. was supported by a grant from the Goldwyn Fund at Brandeis University. We thank W. Carlson for helpful discussions and critical reading of this manuscript.

23 December 1994; accepted 3 May 1995

Rational Design of Peptide Antibiotics by Targeted Replacement of Bacterial and Fungal Domains

Torsten Stachelhaus, Axel Schneider, Mohamed A. Marahiel*

Peptide synthetases involved in the nonribosomal synthesis of peptide secondary metabolites possess a highly conserved domain structure. The arrangement of these domains within the multifunctional enzymes determines the number and order of the amino acid constituents of the peptide product. A general approach has been developed for targeted substitution of amino acid–activating domains within the *srfA* operon, which encodes the protein templates for the synthesis of the lipopeptide antibiotic surfactin in *Bacillus subtilis*. Exchange of domain-coding regions of bacterial and fungal origin led to the construction of hybrid genes that encoded peptide synthetases with altered amino acid specificities and the production of peptides with modified amino acid sequences.

Peptide secondary metabolites produced by microoganisms exhibit diversity with respect to chemical structure and biological activity. These metabolites include antibiotics, enzyme inhibitors, plant and animal toxins, and immunosuppressants and therefore are of importance to medicine, agriculture, and biological research (*1*). Two mechanisms of amino acid incorporation into the bioactive peptides have been identified. The multicyclic lantibiotics, for example, are synthesized ribosomally from gene-encoded peptide precursors, which are extensively modified by complex posttranslational processing (*1*). Other peptides are synthesized on protein templates by a nonribosomal mechanism. This group contributes to the structural diversity of peptide secondary metabolites. These peptides may be composed of linear, cyclic, or branched peptide chains and may contain D-, hydroxy-, or *N*-methylated amino acids that may be modified by acylation or glycosylation (*1*, *2*).

Common to these peptides is their mode of synthesis by multifunctional enzymes that use a thiotemplate mechanism and differ in substrate specificity and size (*2*–*6*). Distinct domains represent the functional building units of these multifunctional enzymes that are responsible for specific amino acid activation (including adenylation and thioester formation), modification, and peptide bond

Biochemie/Fachbereich Chemie, Philipps-University of Marburg, D-35032 Marburg, Germany.

*To whom correspondence should be addressed.

formation (Fig. 1) (*1*–*7*). This type of building block arrangement implies that a synthetase that contains the appropriate number of activating units in the correct order could synthesize any defined peptide.

Sequence analysis of many bacterial and fungal genes encoding peptide synthetases has shown the presence of distinct and homologous domains (Fig. 1A) (*3*). Essential for the design of new, more efficient or less toxic peptides was the identification of functional modules involved in substrate activation as targets for directed modification and alteration of substrate specificity. Recent biochemical and genetic studies have delineated the minimal size of a domain and have defined the location of integral functional modules (Fig. 1A) (*7*). These findings made possible the amplification of specific domain-coding regions, responsible for amino acid recognition and activation, from a diverse group of bacterial and fungal genes encoding peptide synthetases.

Here, we used amplified domains (Table 1) to make specific changes within the *srfA* operon responsible for the biosynthesis of the lipopeptide antibiotic surfactin in *B. subtilis* (*5*). For the creation of hybrid genes, we amplified by polymerase chain reaction (PCR) the coding regions of the Phe-, Orn-, and Leu-activating domains of the *grs* operon from *Bacillus brevis* (*3*) and the Cys and Val domain of the *acvA* gene from *Penicillium chrysogenum* (*6*) (Table 1) (*8*). By cloning these domain-coding regions of bacterial and fungal origin between the linkers of the integration vector pJLA;5′-3′-SRF (Fig. 2, A and B) (*9*, *10*), we constructed gene fusion proteins encoding SrfA-C derivatives whose altered amino acid specificities were determined by the substituted domains (Fig. 2B). The derived fusion proteins are under the control of a heat-inducible promoter and were expressed in *Escherichia coli*. In agreement with results obtained with the wild-type enzyme, these studies revealed recombinant proteins of about 145 kD (*5*), which were detected in protein immunoblots (Fig. 2C).

The *srfA*-C–directed reprogramming of the *srfA* operon in the chromosome of *B. subtilis* was accomplished by gene disruption and replacement, as monitored by a selectable marker. This approach involves two successive steps: marking the chromosomal target site (Leu domain of *srfA*-C) (Figs. 1 and 3) with the selectable gene by double cross-over and delivering an engineered hybrid gene into the marked chromosome by marker exchange. First, the constructed plasmid pSRF-ΔLeu (Fig. 2B) (*9*, *10*) was transformed into the surfactin producer strain *B. subtilis* [American Type Culture Collection (ATCC) number 21332] (*11*). Southern (DNA) blots revealed that several chloramphenicol-resistant (Cm^R) clones that did not

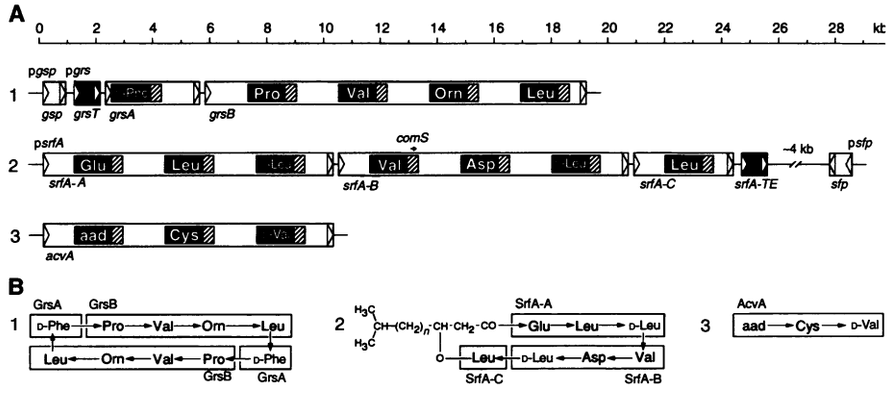

Fig. 1. Multidomain structure of peptide synthetases. (**A**) Schematic diagram of the highly conserved and ordered domain organization of peptide synthetases encoded by the bacterial operons *grs* (row 1) and *srfA* (row 2), and the fungal gene *acvA* (row 3) [aad, δ-(L-α-aminoadipyl)] (*3*, *5*, *6*). The homologous domains are each about 650 amino acid residues in length and contain modules involved in amino acid–specific adenylation (black boxes) and thioester formation (shaded boxes) (*7*). They are separated by nonhomologous regions (white areas). The locations of promoters (p) and genes associated with antibiotic production (*gsp*/*sfp*, *grsT*/*srfA-TE*, and *comS*) are indicated (*3*, *5*, *17*, *19*). (**B**) Primary structure of the nonribosomally synthesized peptides gramicidin S (row 1), surfactin (row 2), and the tripeptide δ-(L-α-aminoadipyl)-cysteinyl-D-valine (ACV), an intermediate of penicillins and cephalosporins (row 3). The amino acid sequences and enzymes that catalyze peptide synthesis are shown.

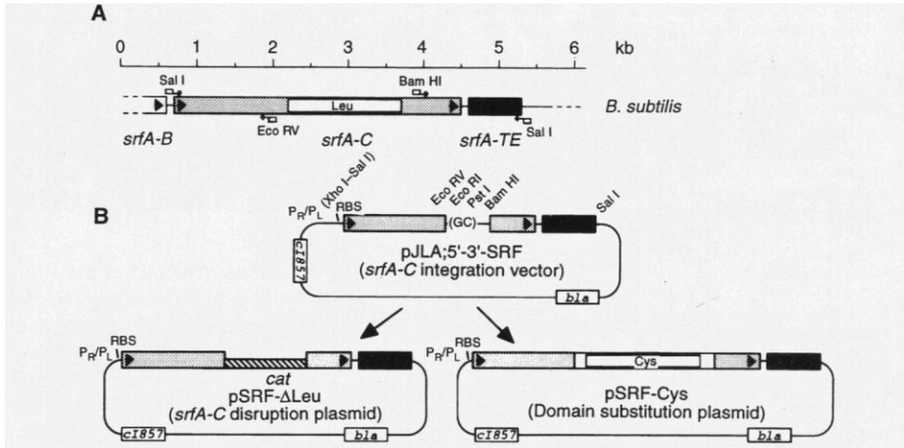

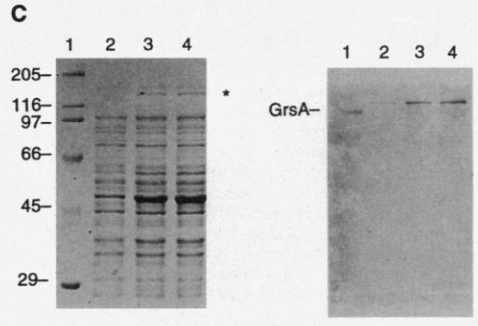

Fig. 2. Construction of hybrid genes encoding SrfA-C derivatives. (**A**) SrfA-C, a leucine-activating 144-kD enzyme, is encoded by the third open reading frame, *srfA-C*, of the surfactin biosynthesis operon (see Fig. 1) (*5*). The domain-flanking regions of *srfA-C* were amplified (*8*), and the resulting two 1.4-kb fragments were cloned into pBluescript with the GC-tailing technique (*16*). (**B**) The amplified fragments were used for the construction of the integration vector pJLA;5′-3′-SRF (*9*), which was used for subsequent, *srfA-C*–directed marker exchange reactions. RBS, ribosomal binding site. Cloning of the *cat* cassette, mediating chloramphenicol resistance, between the linker fragments of pJLA;5′-3′-SRF led to the construction of the *srfA-C* disruption plasmid pSRF-ΔLeu (*9*, *10*). Otherwise, the cloning of domain-coding regions of bacterial and fungal origin (see Table 1) (*9*, *10*) resulted in different domain substitution plasmids (for instance, pSRF-Cys) (Fig. 2B). The resulting *srfA-C* domain fusion genes are under the control of a heat-inducible tandem promoter (P_L/P_R) and could be checked for expression and correct length of the fusion proteins in *E. coli* (*10*, *20*). (**C**) Expression of the hybrid gene *srfA-C(Cys)* (asterisk) was analyzed on a 10% SDS-polyacrylamide slab gel (*20*). The Coomassie-stained gel (left) shows total cell extracts of *E. coli* (pSRF-Cys) at t_0 (lane 2), as well as 1 (lane 3) and 3 (lane 4) hours after heat induction. A commercially available marker (left) and the partially purified GrsA (123 kD) protein (right) were used as markers (lane 1). Both the stained gel and the corresponding protein immunoblot (right) revealed the expression of a protein of ~145 kD (*20*), which coincides with the expected chimeric peptide synthetase.

produce surfactin carried the 1.3-kb *cat* cassette at the chromosomal location of the 1.9-kb domain-coding region of *srfA*-C (Fig. 3A). One clone was chosen for further work and designated TS30.

Next, the plasmids containing domain substitutions—for example pSRF-Cys (Fig. 3A) (*10*)—were used to transform TS30 in order to substitute the desired domain for the *cat* cassette by marker exchange. Exchange was achieved by congression with the plasmid pNEXT33A (*11*). Neomycin-resistant cells (Neo^R) were selected and screened for chloramphenicol sensitivity. About 0.1% to 1% of the transformants had the desired phenotype, and these were tested for the correct insertion of the incoming hybrid genes into the genetically marked chromosome of *B. subtilis*. Southern blots showed that the derived clones were double recombinants in which the distinctive domain-coding regions had been inserted into the *srfA* operon in place of the *cat* gene (Fig. 3B). Successful substitutions were carried out for three bacterial domains from the *grs* operon of *B. brevis* and the two fungal domains of the *P. chrysogenum acvA* gene (Table 1).

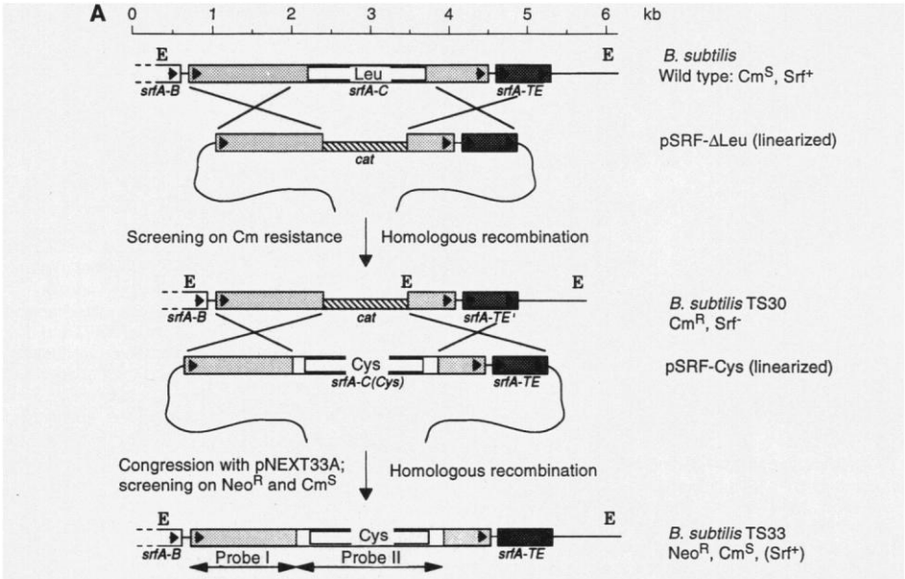

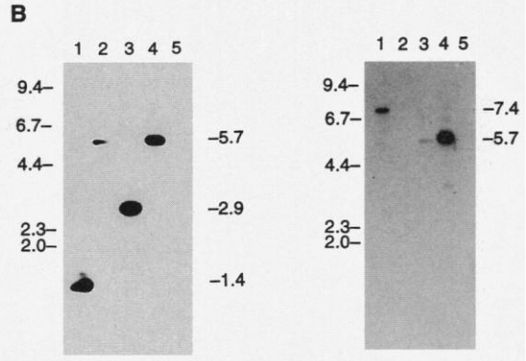

Fig. 3. Targeted *srfA-C* replacement in *B. subtilis*. (**A**) The integrative plasmids constructed (Fig. 2B) were used for in vivo *srfA-C* disruption and domain substitution within the chromosome of *B. subtilis*. Two steps were required: first, the *srfA-C* gene of *B. subtilis* (ATCC 21332) was disrupted by homologous recombination with the linearized plasmid pSRF-ΔLeu (*11*). Subsequently, a domain substitution was achieved by a marker exchange reaction, mediated by the desired domain substitution plasmid (for instance, pSRF-Cys) bearing the gene of a hybrid synthetase (*11*). Loss of the *cat* cassette and the unlinked cotransformation (congression) with pNEXT33A, mediating neomycin resistance (Neo^R), were used to identify strains carrying domain replacements (*11*). Cleavage sites of the restriction enzyme Eco RI within the chromosomal location of *srfA-C* are shown (E). Cm^S, chloramphenicol-sensitive. (**B**) Southern blots of Eco RI–digested genomic DNA were probed with the 5′-linker fragment (left panel) and the substituted Cys domain-coding area of *acvA* (right panel) [shown as double-arrows in (A)], respectively (*16*). For a positive control, we used the unlabeled 5′-*srfA-C* fragment (left) and *acvA* (right) (lanes 1). Genomic DNA was prepared from the wild-type strain *B. subtilis* (ATCC 21332) (lanes 2), TS30 (lanes 3), and TS33 (lanes 4) [compare (A)]. Lanes 5 show Hind III–digested λ DNA as a negative control. The patterns confirmed the disruption (TS30) and domain exchange (TS33) by homologous integration, as shown above. Size markers are indicated on the sides of the gels in kilobases.

The natural surfactin yielded peaks at a mass-to-charge ratio (*m/z*) of 1009, 1023, and 1037, as expected from the known sequence with slight variations in the length of its β-hydroxy fatty acid moiety (n = 7 to 10) (compare Fig. 1B). These $[M+H]^+$ peaks were accompanied by corresponding $[M+Na]^+$ signals appearing at *m/z* 1032, 1046, and 1060 (Table 1) (*15*). Table 1 summarizes the data for the major $[M+H]^+$ peaks obtained from the different surfactin derivatives. Comparison of these data with those for the wild type clearly indicates the replacement of the original Leu^7 residue by the various amino acids, as deduced from the expected sequences of these modified lipopeptides (Table 1). For example, in the mass spectra of the [Cys^7]surfactin (Fig. 4), for each of the various lipid moieties the corresponding peaks of the isoform show values that are 10 daltons less, matching the difference between the molecular masses of the amino acids leucine and cysteine.

The wild-type lipopeptide antibiotic surfactin is a powerful biosurfactant and as such has many potential industrial applications (*13*). A simple test to evaluate its biological activity is the lysis of erythro-

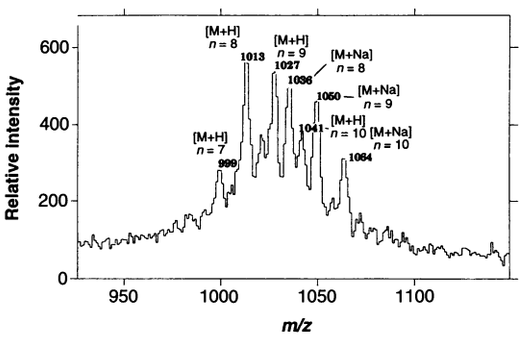

Fig. 4. Mass spectra of engineered [Cys^7] surfactin (*14*). The cyclic lipoheptapeptide appears as a complex mixture of several isoforms that show variations in the length of their β-hydroxy fatty acid moiety (n = 7 to 10 CH_2 groups) (Fig. 1B). The $[M+H]^+$ peaks at *m/z* 999, 1013, 1027, and 1041 were accompanied by the corresponding $[M+Na]^+$ peaks (*m/z* 1036, 1050, and 1064). Comparison of these data with the molecular masses of the wild-type surfactin confirmed the replacement of the Leu^7 residue by Cys in the constructed strain TS33.

Table 1. Summary of domain exchanges in *srfA-C*. The numbers in the domain indicate the location of the domain-coding regions within the DNA sequence of the corresponding gene, as reported for *srfA* (*5*), *grs* (*3*), and *acvA* (*6*). Hemolytic activity (Hem. act.) was monitored on blood agar plates as described (*13*). MS, mass spectra; *E. c.*, *E. coli*; *B. s.*, *B. subtilis*. The Phe domain originates in the *grsA* gene; the Orn and Leu domains originate in the *grsB* genes.

Domain	Expression* in		Hem. act.	MS data† (major peaks)	Peptide product
	E. c.	*B. s.*			
			B. subtilis (*wild-type* srfA-C)		
Leu (22960–24850)	+	+	+	1023,1037	[Leu^7]surfactin
ΔLeu7 (22960–24850)	–	–	–	928, 942	[ΔLeu^7]surfactin, linear
			B. brevis (grs)		
Phe (1890–3760)	+	+	+	1057,1071	[Phe^7]surfactin
Orn (12770–14670)	+	+	+	1024,1038	[Orn^7]surfactin
Leu (15920–17790)	+	+	+	1023,1037	[Leu^7]surfactin
			P. chrysogenum (acvA)		
Cys (5280–7180)	+	+	+	1013,1027	[Cys^7]surfactin
Val (8490–10460)	+	+	+	1009,1023	[Val^7]surfactin

*Expression was tested by protein immunoblot analysis as described (*20*). †Molecular weights have been determined from mass spectra derived for the various lipopeptides extracted (*12, 14*).

cytes. To investigate the influence of the amino acid substitutions on hemolytic activity, we analyzed the extracted surfactins on blood agar plates (*13*). The consequence of *srf*A-C disruption was the complete loss of this activity, whereas the engineered biosurfactants, generated by domain exchanges, restored biological activity. However, in all cases the extent of erythrocyte lysis was slightly reduced compared to that in wild-type peptide (*15*).

Our approach permits the construction of hybrid genes encoding peptide synthetases with altered amino acid specificities. Such engineered genes can be introduced by homologous recombination into the target site of the desired antibiotic biosynthesis operon and cause a programmed alteration within the peptide product. This approach represents a method for the in vivo generation of peptides, allowing the specific engineering of potentially useful secondary metabolites.

REFERENCES AND NOTES

1. F. Lipmann, *Adv. Microbiol. Physiol.* **21**, 227 (1980); M. A. Marahiel, *FEBS Lett.* **307**, 40 (1992); P. Zuber, M. M. Nakano, M. A. Marahiel, in Bacillus subtilis *and Other Gram-Positive Bacteria,* A. L. Sonenshein, J. A. Hoch, R. Losick, Eds. (American Society for Microbiology, Washington, DC, 1993), pp. 897–916.
2. T. Stachelhaus and M. A. Marahiel, *FEMS Microbiol. Lett.* **125**, 3 (1995).
3. K. Turgay, M. Krause, M. A. Marahiel, *Mol. Microbiol.* **6**, 529 (1992); J. Krätzschmar, M. Krause, M. A. Marahiel, *J. Bacteriol.* **171**, 5422 (1989).
4. G. Weber, K. Schörgendorfer, E. Schneider-Scherzer, E. Leitner, *Curr. Genet.* **26**, 120 (1994); M. Krause, M. A. Marahiel, H. von Döhren, H. Kleinkauf, *J. Bacteriol.* **162**, 1120 (1985); J. S. Scott-Craig, D. G. Panaccione, J.-A. Pocard, J. D. Walton, *J. Biol. Chem.* **267**, 26044 (1992); A. Haese, M. Schubert, M. Herrmann, R. Zocher, *Mol. Microbiol.* **7**, 905 (1993).
5. P. Cosmina *et al.*, *Mol. Microbiol.* **8**, 821 (1993); S. Fuma *et al.*, *Nucleic Acids Res.* **21**, 93 (1993).
6. D. J. Smith, J. E. Alison, G. Turner, *EMBO J.* **9**, 2743 (1990).
7. T. Stachelhaus and M. A. Marahiel, *J. Biol. Chem.* **270**, 6163 (1995).
8. Amplification of DNA fragments was performed as described (*7*) [K. Turgay and M. A. Marahiel, *Peptide Res.* **7**, 238 (1994)]. The sequences of the oligonucleotide primers were as follows [underlined, modified sequence; bold, restriction site; bracket, location based on sequence data published for *srfA (5)*, *grs (3)*, or *acvA (6)*]: oligo 5′-SrfA-C–Sal I (21560): 5′-AGG G**GT CGA C**AG AAG GCG GGA GCG AAA CAT-3′; oligo 3′-SrfA-C-Eco RV (22960): 5′-CTT TG**G ATA TC**G AGC TTG AGC CGG CGG GTT TAA-3′; oligo 5′-SrfA-C–Bam HI (24850): 5′-CG**G GAT CC**T TGA GGA GGA AGA CCG GCT TGA-3′; oligo 3′-SrfA-C–Sal I (26170): 5′-AAA G**GT CG**A CAG CCG AAG CTG TCC GCT TTT-3′; oligo 5′-Orn/grs–Eco RV (12770): 5′-GC**G GAT ATC** CTA AAA TAT TCC ATG AGT TAT TTG-3′; oligo 3′-Orn/grs–Bam HI (14670): 5′-CG**G GAT CCC** GAG CAT GAT GGA AGG CAT ATT-3′; oligo 5′-Leu/grs–Nru I (15920): 5′-ATA **TCG CGA** ATC AAA CAA TAC AGG AAT TG-3′; oligo 3′-Leu/grs–Bam HI (17790): 5′-TAA **G**GA **TCC** GGA ATA CGT TTC GAT CTG-3′; oligo 5′-Cys/acv–Nru I (5280): 5′-ATT C**TC GCG A**TG TTT GAA AAC GAA GC-3′; oligo 3′-Cys/acv–Bgl II (7180): 5′-TAG **AGA TCT** CAA ATG CAG CGT CGA T-3′; oligo 5′-Val/acv–Pma CI (8490): 5′-ACT **ACA CGT G**AG GAG CAG AAA GTA G-3′; and oligo 3′-Val/acv–Bgl II (10460): 5′-AAC ATA **GAT CT**C TGG CGT TCG GAC-3′. The PCR was carried out in a Perkin-Elmer Thermal Cycler 480 (Perkin-Elmer, Überlingen, Germany), and products were purified with the QIA quick-spin PCR purification kit as described by the manufacturer (Qiagen, Hilden, Germany).
9. Standard procedures were used for the digestion with restriction enzymes, the cloning of DNA fragments, and the preparation of plasmid DNA (*16*). The integrative vector pJLA;5′-3′-SRF was constructed in steps. First, the amplified (*17*) 5′- and 3′-*srfA-C* fragments were cloned into the Eco RV–digested vector pBluescript by the GC-tailing technique (*16*). The 3′-linker was prepared from the resulting plasmid, making use of the PCR-generated restriction sites Bam HI and Sal I, and subcloned into the *E. coli* expression vector pJLA503 (Medac, Hamburg, Germany) digested with the same enzymes. Subsequently, the 5′-*srfA-C* fragment was prepared, with the use of the 5′-generated restriction site Sal I and the unique Bam HI restriction site of the vector. The 1.4-kb fragment was subcloned in the Xho I–Bam HI–digested vector pJLA;3′-SRF, and this step resulted in the *srfA-C* integration vector, designated pJLA;5′-3′-SRF (Fig. 2B).
10. The gene disruption plasmid and the domain substitution plasmids were cloned with the Eco RV–Bam HI–digested integration vector pJLA;5′-3′-SRF, a 1.4-kb Eco RV–Bam HI fragment of pDG268 [C. Antoniewski, B. Savelli, P. Stragier, *J. Bacteriol.* **172**, 86 (1990)] bearing *cat*, or an amplified domain-coding region bearing compatible terminal restriction sites (*8, 9*). The cloned *grsA* fragment, containing the Phe domain-coding region, was prepared from pMK21 (*3*) with the endonucleases Pma CI and Bgl II (*16*). We verified the constructed genes by sequencing the junctions between the vector and the inserted, domain-coding fragment, using the chain termination method. [F. Sanger, S. Miklen, A. R. Coulson, *Proc. Natl. Acad. Sci. U.S.A.* **74**, 5463 (1977)]. The sequences of the primers used were as follows: oligo 5′-SRF (22810): 5′-GAT GAG GCG TTT ATC CTG-3′; oligo 3′-SRF (24950): 5′-GCA GCT TCA AAC GCC AGG C-3′.
11. Transformation of *B. subtilis* was performed by a two-step method as described (*18*). For congression experiments, we used pNEXT33A as a carrier of the unlinked selection marker *neo* [M. Itaya and T. Tanaka, *Mol. Gen. Genet.* **223**, 268 (1990)]. The transformants were selected on 2× yeast tryptone (YT) medium containing neomycin (10 μg/ml).
12. For the extraction of surfactin, *B. subtilis* strains were grown in SpC medium (*18*) at 33°C and 300 rpm for 48 hours. Cells were collected by centrifugation for 15 min at 6000*g*, and the culture broth was mixed with trichloroacetic acid to a final concentration of 5%. We filtered the suspension through an RC58 membrane filter (Schleicher & Schuell, Dassel, Germany), washed the remainder with 5% trichloroacetic acid, 1 mM hydrochloric acid, and water, and air-dried the residual lipopeptide. Finally, the surfactin was dissolved in ethanol by shaking at 4°C. The time courses of production of the altered surfactins were comparable to those of the wild type, although at a reduced level.
13. M. M. Nakano, M. A. Marahiel, P. Zuber, *J. Bacteriol.* **170**, 5662 (1988); D. G. Cooper, *Microbiol. Sci.* **3**, 145 (1986).
14. Mass spectrometry was carried out by the plasma desorptions technique (PDMS) performed by R. Weber and H. Jungclas (Abt. Klinische Nuklearmedizin, FB20, Philipps-University of Marburg, Germany).
15. T. Stachelhaus, A. Schneider, M. A. Marahiel, data not shown.
16. J. Sambrook, E. F. Fritsch, T. Maniatis, *Molecular Cloning: A Laboratory Manual* (Cold Spring Harbor Laboratory, Cold Spring Harbor, NY, 1989).
17. M. M. Nakano, N. Corbell, J. Besson, P. Zuber, *Mol. Gen. Genet.* **232**, 313 (1992); S. Borchert, T. Stachelhaus, M. A. Marahiel, *J. Bacteriol.* **176**, 2458 (1994).
18. S. M. Cutting and P. B. Vander Horn, in *Molecular Biological Methods for* Bacillus, C. R. Harwood and S. M. Cutting, Eds. (Wiley, Chichester, UK, 1990).
19. C. D'Souza, M. M. Nakano, P. Zuber, *Proc. Natl. Acad. Sci. U.S.A.* **91**, 9397 (1994); L. W. Hamoen, H. Eshuis, J. Jongbloed, G. Venema, D. van Sinderen, *Mol. Microbiol.* **15**, 55 (1994).
20. *srfA-C* substitution plasmids allow the expression of the cloned hybrid genes under control of the bacteriophage λ promoters P_R and P_L in tandem, which are regulated by a heat-sensitive repressor clts857. Cells were grown at 28°C and 300 rpm until the absorbance at 600 nm reached 0.8. The temperature was shifted to 42°C, and the cultures were grown for an additional 3 hours. *Bacillus subtilis* cells were grown in Difco sporulation medium (*13*). In both cases, expression of the hybrid synthetases was analyzed by SDS–polyacrylamide gel electrophoresis [U. K. Laemmii, *Nature* **227**, 491 (1970)] and protein immunoblotting [H. Towbin, T. Stachelin, J. Gordon, *Proc. Natl. Acad. Sci. U.S.A.* **76**, 4350 (1979)], with antibodies raised against the Phe or Pro domain of the gramicidin S biosynthetic system.

21. We wish to thank R. Weber and H. Jungclas for the realization of the mass spectrometrical studies and I. Schüler for technical assistance. We appreciate the expert and valuable comments of R. Losick, D. Sherman, and M. Yudkin and thank G. Turner for providing *acvA*. Supported by the Deutsche Forschungsgemeinschaft and the Fond der chemischen Industrie.

6 March 1995; accepted 3 May 1995